Original Article

A Novel ODMC Model for Malaria Blood Smear Classification using Deep Feature Fusion and Optimization

Talha Imran[1], Saman Iftikhar[2]*, Kiran Fatima[3], Malak ElAmir[4], Noof Abdulaziz Alansari[5], Ammar Saeed[6]

[1]Department of Computer Science, COMSATS University Islamabad, Wah Campus, Wah Cantt, Pakistan, 47040
Email: itsmetalhaimran@gmail.com
[2]Faculty of Computer Studies, Arab Open University, Riyadh 11681, Saudi Arabia.
Email: s.iftikhar@arabou.edu.sa
[3]Technical and Further Education (TAFE), New South Wales (NSW), Australia.
Email: kiran.fatima4@tafensw.edu.au
[4]Faculty of Computer Studies, Arab Open University, Riyadh 11681, Saudi Arabia.
Email: melamir@arabou.edu.sa
[5]Faculty of Computer Studies, Arab Open University, Riyadh 11681, Saudi Arabia.
Email: n.alansari@arabou.edu.sa
[6]Department of Computer Science, COMSATS University Islamabad, Wah Campus, Wah Cantt, Pakistan, 47040.
Email: ammarsaeed1997@gmail.com

Abstract

Background: Malaria poses an enormous threat to humanity with ever increasing cases annually. The research in the field of medical is contributing quite a lot in providing methods for premature diagnosis of malaria. Apart from medical research, information technology is also playing a vital role in proposing efficient methods for malaria diagnosis. **Aim:** To minimize the manual interference and boost the diagnosis accuracy, the automated systems are under study lately. In the proposed work, an Optimized Deep Malaria Classifier (ODMC) is proposed for accurate and efficient malaria blood smear classification. **Method:** A dataset comprising of healthy and infected images of malaria blood smears is preprocessed using color space transformation and a series of other image enhancement steps. The deep features are extracted using the well-trained layers of pre-trained Convolutional Neural Networks (CNNs) including ResNet101(RSN101) and SqueezeNet (SQN). Apart from this, the local handcrafted features are also extracted from the preprocessed dataset using Local Binary Patterns (LBP). Both the deep features and the handcrafted features are serially fused together to formulate a compact feature vector which is then optimized using Linear Discriminant Analysis (LDA). The optimized vector is the classified using multiple classifier kernels. **Results:** The ODMC achieved 99.73% accuracy and 99.76% precision whilst maintaining an efficient prediction speed and training time.

Keywords: Malaria, Medical Imaging, ODMC Model, Deep Learning, Transfer Learning, Feature Fusion, Feature Optimization, CNN, Classification.

Introduction

Malaria is one of the most significant public health challenges globally, especially in regions with hot, humid climates where the Anopheles mosquito thrives. The disease is caused by the transmission of Plasmodium parasites through the bites of infected mosquitoes. Among the five Plasmodium species that infect humans, Plasmodium falciparum and Plasmodium vivax are particularly deadly, leading to severe health complications and high mortality rates.[1] The prevalence of malaria is staggering, with over 210 million cases reported in more than 90 countries by the end of 2016. Alarmingly, this number rose to 228 million cases worldwide by 2018, highlighting the persistent threat that malaria poses to global health.[2] In addition to its widespread prevalence, malaria is responsible for significant mortality, particularly among vulnerable populations such as young children. In 2018 alone, an estimated 405,000 people died from malaria, with children under five years of age accounting for 67% of these deaths. The burden of malaria is disproportionately high in sub-Saharan Africa, which accounts for 93% of all malaria cases and

Access this article online

Quick Response Code:

Website: www.jnsbm.org

DOI: https://doi.org/10.4103/jnsbm.JNSBM_15_2_23

Address for Correspondence: Faculty of Computer Studies, Arab Open University, Riyadh11681, Saudi Arabia
Email: s.iftikhar@arabou.edu.sa

Submitted: 15th July, 2024 **Received:** 27th August, 2024
Accepted: 05th September, 2024 **Published:** 16th September, 2024

How to cite this article: Imran T, Iftikhar S, Fatima K, ElAmir M, Alansari N A, Saeed A. A Novel ODMC Model for Malaria Blood Smear Classification using Deep Feature Fusion and Optimization. J Nat Sc Biol Med 2024;15:376-388

94% of malaria-related deaths globally.[3] These statistics underscore the urgent need for effective malaria control and prevention strategies.

Traditional malaria diagnosis relies on the manual examination of blood smears under a microscope by skilled technicians. This process, while effective, is time-consuming and labor-intensive. Accurate parasite detection and quantification are crucial for proper diagnosis, treatment, and monitoring of disease progression. However, the manual nature of this process introduces variability and the potential for human error, which can lead to misdiagnosis, incorrect treatment, and ultimately, poor patient outcomes.[4] Factors such as the experience of the technician, the quality of the microscope, and environmental conditions can all impact the accuracy of the diagnosis. Given the limitations of manual diagnosis, there has been a growing interest in the development of automated systems that can assist or even replace human technicians in the diagnosis of malaria. Recent advancements in machine learning and deep learning have opened new avenues for developing such automated systems. These technologies have demonstrated remarkable success in various medical imaging applications, including skin cancer detection, brain tumor segmentation, and liver disease classification.[5] By leveraging the power of deep learning, it is possible to develop models that can analyze blood smear images with high accuracy and efficiency.

In this study, we address the critical need for an automated, accurate, and efficient malaria diagnosis system by proposing an Optimized Deep Malaria Classifier (ODMC). The primary objective of our research is to develop a novel feature fusion-based model that combines the strengths of state-of-the-art deep Convolutional Neural Networks (CNNs) with handcrafted texture features. Specifically, our approach integrates deep features extracted from ResNet101 and SqueezeNet, two well-established CNN models, with low-level texture features derived from Local Binary Patterns (LBP). This fusion of deep and handcrafted features is designed to enhance the model's ability to discriminate between healthy and infected blood smear images, leading to improved diagnostic accuracy. The specific aims of our study include:

- Developing a robust feature fusion strategy that effectively combines deep and handcrafted features to capture both high-level and low-level information from blood smear images.
- Implementing an advanced image preprocessing technique that enhances image contrast by mapping the images to the HSV color space and separately adjusting the Hue, Saturation, and Value channels. This preprocessing step is intended to improve the quality of the input images, thereby boosting the performance of the ODMC model.
- Employing LDA to optimize the fused features, reducing their dimensionality and mitigating the risk of overfitting. This optimization process is crucial for ensuring that the model remains both accurate and computationally efficient.
- Evaluating the performance of the ODMC model using a set of classifiers to determine its accuracy, efficiency, and potential for real-world application.

The research questions guiding this study are:

- How does the fusion of deep learning features with handcrafted texture features improve the accuracy and robustness of malaria diagnosis from blood smear images?
- What role do image preprocessing techniques, such as HSV color space mapping, play in enhancing the diagnostic accuracy of deep learning models?
- How well can the fusion of multiple CNN models and a handcrafted feature extractor assist in accurate classification of malaria blood smear classification?
- How effective is a feature optimization algorithm such as LDA in optimizing feature selection, reducing overfitting, and improving the overall performance of the ODMC model?

By addressing these research questions, our study aims to contribute to the development of reliable and efficient automated systems for malaria diagnosis. The proposed ODMC model, which integrates deep learning with traditional image processing techniques, has the potential to significantly improve the accuracy and efficiency of malaria diagnosis, ultimately reducing the burden of this deadly disease on global health. With an accuracy rate of 99.73%, our ODMC model demonstrates its capability as a highly effective tool in the fight against malaria.

Related Work

Accurate malaria blood smear diagnosis and classification is an active research area in the field of medical imaging. Many works have been proposed in the field of malaria diagnosis till now. The work[6] addresses the challenge of detecting rouleaux formation, a common red blood cell abnormality that complicates malaria diagnosis. The authors collected 231 images each of normal and rouleaux-affected blood cells, creating a dataset of 3044 segmented images. Two CNN models were developed and trained to classify these images. The first model achieved a validation accuracy of 87.91% with 300x300 pixel images, while a second model using depthwise separable CNN layers improved accuracy to 90.95%. This study highlights the importance of image size in optimizing model performance and contributes a new dataset to aid in developing more robust automated malaria diagnostic systems capable of detecting both parasites and blood cell abnormalities.

The authors[7] present an Optimal Machine Learning-based Automated Malaria Parasite Detection and Classification (OML-AMPDC) model, designed to address challenges in malaria diagnosis, such as limited expert availability and poor image quality. The model starts with preprocessing steps that include adaptive filtering for noise removal and contrast enhancement using the CLAHE technique. Features are extracted

using Local Derivative Radial Patterns (LDRP), and classification is carried out using a Random Forest (RF) classifier. To optimize the RF classifier's performance, the Particle Swarm Optimization (PSO) algorithm is employed, specifically tuning parameters like max_ depth and n_estimators. Experimental results using a benchmark dataset demonstrate that the OML-AMPDC model outperforms recent approaches in malaria parasite detection and classification. Shi *et al.*[8] utilized plasmodium cell images from Central South Hospital, Wuhan University. Dataset augmentation is performed with the help of arbitrary point revolution, horizontal and vertical flipping, Gaussian blur and contrast improvement. Variable edge detection is utilized to recognize distorted images. Enhanced image information is given to the fused neural network architecture including Inception V3, Resnet 50 and Inception V2 which performs feature learning and makes a component vector subsequently. Pattanaik *et al.*[9] utilized 1150 cell images acquired from high end magnifying microscope and regular cell phones at different amplification scales. The pre-processing is done by resizing images obtained at 1000x amplification into 50x50 pixels impeccable square dimension. Images obtained at 750x750 pixels are also field stained and examined at x1000 amplification. A novel system is put together which comprises of FLANN based CAD model for feature extraction, Stacked Sparse Autoencoder (SSAE) model is utilized to restrain the highlights relying upon measurement and concealed layers.

The research[10] addresses the critical need for early and accurate malaria diagnosis by introducing two deep learning algorithms specifically designed for malaria classification. The first algorithm utilizes a binary classifier convolutional neural network (CNN) model, achieving an accuracy of 90.20%. The second, a customized CNN model, demonstrates an even higher accuracy of 96.02%. These models were developed to improve the precision and efficiency of malaria diagnosis, especially in regions where expert microscopists are scarce. The study highlights the superior performance of these models compared to existing methods, underscoring their potential to enhance automated malaria detection and reduce global mortality rates associated with the disease. Rajaraman *et al.*[11] used dataset containing 27,558 parasitized and healthy cell images from Kaggle. Squeezing layer of the SqueezeNet along with channels of differing sizes is used for feature learning and extraction. Global Average Pooling (GAP) is utilized for dimensionality reduction. Three convolution layers and two fully connected layers are implemented completely in the DL model for feature learning.

Vijayalakshmi *et al.*[12] resized the images to 224 pixels' dimension with uniformity of 100dpi and utilized mean and variance filters for preprocessing. Improved images from preprocessing are given to CNN with no further change. Pooling layers and fully connected layers are used in the pretrained VGG model to perform feature extraction. The two CNN models VGG-16 and VGG-19 are reused with changes by joining them with SVM classifier to make a VGG-SVM Model. Abbas *et al.*[13] utilized powerful Dynamic Convolutional Filtering (DCF) to segment parasitized parts of cells. Intensity based highlights, color highlights, texture highlights, LBP and HSV highlights are among the prominent elements in the feature extraction stage. Abbas *et al.*[14] used adaptive gaussian mixture based dynamic segmentation to segment the affected parts based on color grading and intensity for the isolation of parasitized malaria cells.

Yang *et al.*[15] used parasite screening and WBC extraction based on histogram intensities of the grayscale images utilizing Otsu's segmentation technique. Force highlights and shading highlights are utilized in the preprocessing stage and later on convolutional layers alongside fully connected layers are utilized to separate all the areas of interest. Modified CNN including 7 convolution layers, three pooling layers, three fully connected layers and a delicate layer has been proposed. Santosh *et al.*[16] predicted malaria affected regions based on 4 Geographical locations & Rural health centers. Multivariate imputation is used by the chained equation to handle the missing data points from environmental data. The multivariate imputed data is passed on to LSTM classifier for prediction of a certain period. The study[17] introduces an AI-based object detection system for malaria diagnosis, named AIDMAN, which leverages advanced deep learning techniques to improve the accuracy and efficiency of malaria detection, particularly in resource-limited areas. AIDMAN uses the YOLOv5 model for detecting cells in thin blood smears, followed by an attentional aligner model (AAM) for cellular classification and a CNN classifier for diagnosis. The system achieves an impressive diagnostic accuracy of 98.62% for individual cells and 97% for blood-smear images. AIDMAN's performance is on par with that of experienced microscopists, making it a promising tool for malaria diagnosis in regions where trained professionals and equipment are scarce. The study highlights the potential of AI to enhance malaria detection, reduce transmission, and ultimately save lives, particularly in high-burden areas like Africa.

The study[18] tackles the challenge of malaria diagnosis, which causes over 500,000 deaths annually. Traditional microscopy, while effective, is slow and prone to errors, highlighting the need for automation. This research employs Convolutional Neural Networks (CNNs) with VGG16 architecture, Transfer Learning, and Adaptive Boosting to analyze microscopic blood slides. The dataset is enhanced through preprocessing to ensure diversity and robust model training. By leveraging transfer learning, the model improves its ability to classify malaria-infected erythrocytes accurately. Addressing limitations of previous CNN-based methods, such as sensitivity and dependence on large datasets, this study incorporates adaptive boosting and hyperparameter tuning. The resulting system achieves over 96% accuracy, providing a reliable, automated solution for malaria

detection in clinical settings. Das et al. [19] performed illumination correction using grayish induction. They performed noise reduction using mean filter based on geometry. Marker controlled watershed segmentation is utilized to segment erythrocytes from microscopic images. Co-occurrence based on gray matrix GLCM is used. The purpose is to obtain the texture features including entropy, correlation, space etc. More than 70 textural features & 15 shape features are put into use to differentiate between more than five types of blood cells. Naïve Bayes classifier is used along with SVM to accurately classify malaria infected cells from healthy cells. Malaria diagnosis traditionally relies on manual microscopy, which is time-consuming and prone to error. To improve accuracy and efficiency, an ensemble deep learning model has been developed[19] using retrained VGG16, VGG19, and DenseNet201 networks, combined with adaptive weighted averaging and max voting techniques. This model, enhanced with data augmentation and various image processing methods, achieves a diagnostic accuracy of 97.92% for identifying malaria parasites in red blood cell images, offering a promising automated solution for more reliable and efficient malaria detection.

Proposed Methodology

In this study, we propose a novel ODMC model that integrates deep learning and handcrafted features to enhance malaria detection. The model combines features learned from the deep learning models RSN-101 and SQN with textural features extracted using LBP. To improve image quality, we apply a contrast enhancement technique in the HSV color space, adjusting the hue, saturation, and value channels separately, which makes the infected regions more prominent. The images are resized to a uniform dimension of 224 pixels to maintain consistency. The deep learning models are trained on RGB images, while the LBP features are extracted from grayscale images. These features are then concatenated and optimized using LDA, which selects the most significant features based on interclass and intraclass variance, thus reducing computational complexity and enhancing classification accuracy. The final features are classified using various classifiers, resulting in an impressive accuracy of 99.73%, demonstrating both high efficiency and accuracy in malaria diagnosis.

The workflow of proposed model is shown in Figure 1. The functioning of proposed model is discussed in detail with respect to all the steps data acquisition, preprocessing, feature extraction and optimization, and classification in coming sections.

Data Gathering and Preparation

Data gathering and preparation are the primary tasks of our proposed work as all the upcoming steps are dependent on them. Both the steps are discussed in the separate sections below.

Data Collection

The dataset used in this work is obtained from Kaggle which originally contains 27,558 blood smear images divided into two classes namely parasitized and uninfected with each class containing 13,779 images. The images are in RGB color channel and varying in terms of scale as shown in Figure 2.

Data Preparation and Preprocessing

Preprocessing is a very crucial step in any image analysis problem due to its massive impact on the end result. Several preprocessing steps are employed in this work as well to make our model better deduct information from malaria affected images. Initially, all the images are in different scales and sizes which creates biasness and mislead results due to which they are resized into 224-pixel dimension which resolves this problem. The dataset images are also converted to 2-dimesional grayscale channel to utilize them in LBP which takes grayscale images as input as shown in Figure 2.

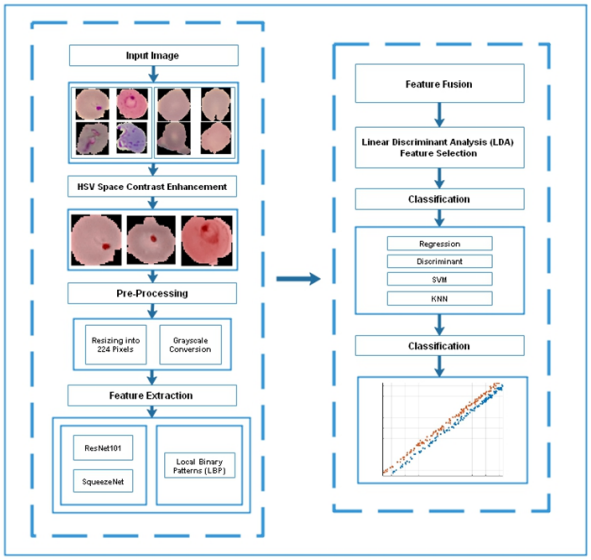

Figure 1: ODMC Workflow Architecture.

Color grading improvement and contrast enhancement are widely utilized approaches in the field of medical imaging as they amplify the crucial information in the targeted images and increase the gross quality of images. Better quality images are more likely to provide better results as they assist proposed model in terms of clarity and interpretation. Various image contrast enhancement techniques are implemented by several works over the time.[20-23] In the proposed work, images are enhanced by converting them to HSV color space and then separately enhancing the hue, saturation and value channel carefully such that the parasitized part of image gets more prominent and highlighted thus making it easier for the proposed model to classify more precisely. The HSV color processing makes the color of defected regions stand out as compared to the rest of image part as shown in Figure 3.

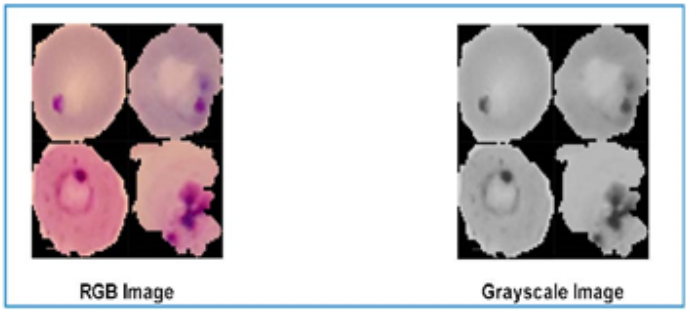

Figure 2: RGB to Grayscale Conversion.

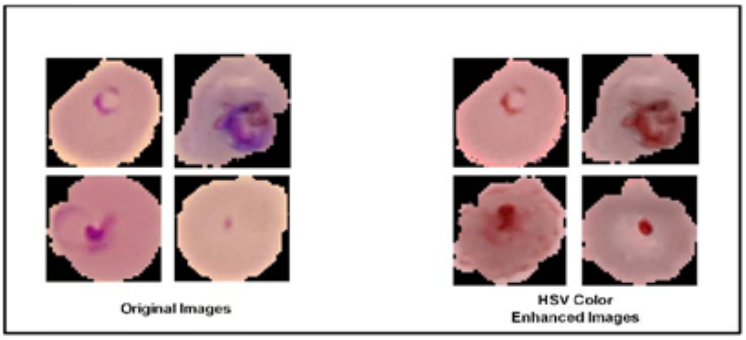

Figure 3: Image Enhancement in HSV Color Space.

Feature Extraction (FE)

After data acquisition and preparation, the next step is to acquire features from it which can be done using either deep learning models or by using a handcrafted feature learner. Numerous techniques have been employed in medical imaging depending on the nature of images and required features. Several works attained color, shape, geometric shape, edge, corner, blob, scale and textural features using different techniques over the course of time to extract suitable information from concerned images.[24-27] In the proposed work, low level features are derived by means of Local Binary Patterns (LBP) and deep features are obtained using two deep CNN models which are discussed in the coming sections.

Low Level Features

LBP has been implemented in many medical imaging, text identification and facial recognition problems in order to derive texture-based features and was first presented in 1994.[28] It has played a vital role in prevailing the vital details from images in many works where it has also been used in merger with many other models and has showed promising results.[29,30] In the suggested work, the images containing malarial parasite symptoms have a varying texture as compared to the rest of the images. Therefore, LBP is utilized to better learn those varying features and assist in finalizing better results. In LBP, a 3x3 mask is utilized and threshold is compared with neighborhood pixels.[31] Image dataset is converted into grayscale and then passed on to LBP which extracts 59 features from 27,558 images given to it. LBP extracts and calculates features using the Equation 1:

$$LBP\ (Q,R) = \sum_{n=0}^{Q-1} k(l_n - l_m)2^n \quad (1)$$

In Equation 1, and represents the starting seed threshold pixel and the adjacent pixels respectively. In this case, the number of Q pixels are chosen for a surrounding area R. Maximum information can be obtained with close distance pixels and this relation decreases as the distance between pixels gradually increases due to which the area radius R is kept fairly small.[32,33]

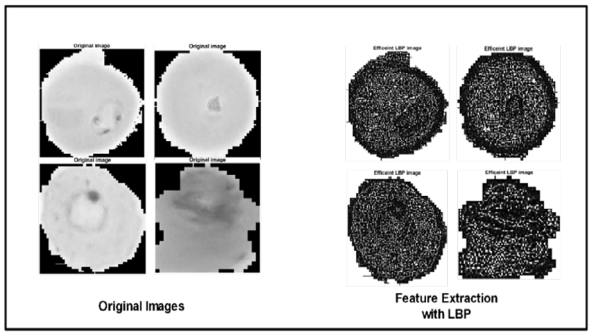

Figure 4: Original Images (Left). Images After Performing LBP Operation (Right).

Figure 4 shows some of the original images and their situation when LBP is operated in them. RGB images are converted into grayscale prior to LBP implementation.

Deep Features

Although, low level features can be useful in many tasks but they have their limitations when presented a larger dataset as they are not deeply learned enough to increment the performance of engineered model. Moreover, a particular handcrafted feature extractor can only draw

out specific type of features for which it is designed and cannot perform all tasks which puts the need of deep feature learning models forward.[34] Deep CNN models have been widely used in all sorts of medical imaging problems where they have outplayed standard feature extraction models in terms of results.[35-39] The proposed work also employs two deep networks ReNet101 and SqueezeNet for feature learning from the dataset images which are discussed in coming sections.

ResNet101 (RSN-101)

It is a CNN which has a 101-layer depth and pretrained on more than a million images from the image net database. RSN-101 has been successfully used for brain tumor classification,[40] detecting covid-19 affected chest CT scans,[41] breast cancer classification[42] and many other medical imaging problems and it has proven to be quite effective which motivates us to implement it in the proposed work as well. The pre-trained ResNet101 takes RGB images in 224-pixel dimension as input and derives 2048 features from the total of 27,558 images. The features are extracted from the pooling layer (pool5) of RSN-101 as there is no need of using the classification layers since classification is going to be performed after fusing the features from other deep networks and LBP at the end using the classification learner. So, the features are obtained and temporarily saved for the time being.

SqueezeNet (SQN)

It is a 18 layers deep CNN model which is pretrained on a million ImageNet repository-based images and has also been employed in many image processing problems including covid-19 diagnosis,[43] gastric precancerous diseases classification,[44] diabetic retinopathy detection.[45] In the proposed model, a total of 27,558 preprocessed images are directed to the SqueezeNet which learns a total of 1000 features out of them. The features are extracted from the pooling layer (pool10) of SQN and temporarily stored in order to merge them with the features of other two deep models after the learning phase is completed. Table 1 shows complete comparison of features obtained from both CNN models as well as the LBP for the same dataset provided to each.

Table 1: Overview of Extracted Features for Proposed Model.

FE	Hand-Crafted	Deep Network	Feature Layer	Images			Total Features
				Parasitized	Un infected	Total	
LBP	Y	-	-	13779	13779	27558	10000x59
ResNet 101	-	Y	Pool5	13779	13779	27558	10000x2048
Squeeze Net	-	Y	Pool10	13779	13779	27558	10000x1000

Feature Fusion and Selection

In this phase, the features extracted by RSN-101 (27558x2048) and SQN (27558x1000) are merged together with the approach of serial feature fusion. This creates a compact package comprising of collective attributes (27558x3048) delivered by both the frameworks constituting both important and non-important attribute vectors and needs to be optimized for better gain of results and complexity handling. LDA has been efficiently implemented in many image processing related tasks for modality classification,[46] feature dimensionality reduction and optimization.[47] In the proposed work, LDA is used as a feature selector which maximizes the variance between different classes and increases separation.

Given two different dataset classes X1 and X2 whose features are represented in the form of matrices in Eq. 2.

$$X1 = \begin{bmatrix} D1_{11} & D1_{12} \\ D1_{21} & D1_{22} \\ \dots & \dots \\ \dots & \dots \\ D1_{n_1} & D1_{n_2} \end{bmatrix} \; X2 \begin{bmatrix} D2_{11} & D2_{12} \\ D2_{21} & D2_{22} \\ \dots & \dots \\ \dots & \dots \\ D2_{n_1} & D2_{n_2} \end{bmatrix} \quad (2)$$

The mean of each data class is calculated individually as well as mean of entire data compilation is also calculated using the sum of all data classes as shown in Eq. 3 where l_1 and l_2 are the inferred probabilities of the classes, M1 and M2 be the mean of class 1 and class 2 individually and M3 is the mean of entire dataset.[48]

$$M_3 = l_1 \, x \, M_1 + \, l_2 \, x \, M_2 \quad (3)$$

LDA works by maximizing the between class variance to the within class variance which is calculated using Eq. 4 and Eq. 5 respectively.

$$V_w = \sum_n l_n \; x \; (var_n) \quad (4)$$

In Eq. 4, V_w represents within class variance and var_n denotes the estimated variance of concerned class.

$$V_b = \sum_n (M_j - M_3) \; x \; (M_j - \; M_3)^T \quad (5)$$

In Eq. 5, V_b represents between class variance, M_j denotes overall mean of all the classes. In the proposed work, LDA takes the fused features with dimensionality (27558x3048) and processes it thus providing a very concise and compendious vector containing absolute relevant attributes from the original detail set with dimension of (27558x6). A clear difference can be seen here between the original input complexity and reduced set compactness which later in classification stage significantly decreases time exertion.

Classification

The final phase in the proposed work is the classification phase where the parasitized and uninfected image features are discriminated from each other. For this purpose, all the selected features are passed on to eight different classifiers and their kernels including Logistic Regression (LR), Linear Discriminant (LD), Quadratic Discriminant (QD), Linear SVM (L-SVM), Cubic SVM (CB-SVM), Coarse Gaussian SVM (CG-SVM), Fine KNN (F-KNN), Coarse KNN (CR-KNN) and Weighted KNN (W-KNN).

The proposed model achieves an excellent accuracy of **97.35** while maintaining efficient time consumption rate.

Experimentation and Results

In this section, all the experiments are demonstrated in detail along with their corresponding results and evaluation measures. The dataset used for the experimentation purpose is also discussed.

Dataset Presentation

The dataset used in this work is originally manufactured and prepared by National Institute of Health (NIH) which originally contains 27,558 red blood cells images obtained from smears. The data compilation is divided among two classes i.e., parasitized and uninfected with 13,779 images in each class. The images are in RGB channel and are slightly varying in terms of scale. The dataset is publicly available at Kaggle[49]. Dataset demonstration is shown in Figure 5.

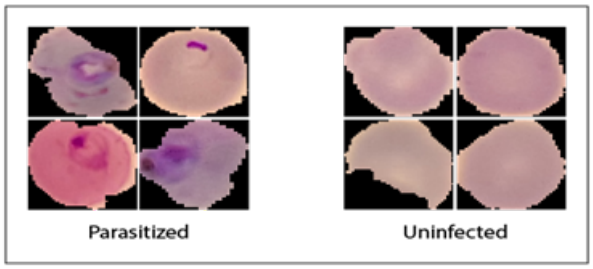

Figure 5: Visualization of Two Dataset Classes.

Performance Evaluation Metrics and Implementation Settings

A few metrics are used for the evaluation of proposed work which include accuracy, precision, sensitivity, recall, specificity, f1 score.[50] Accuracy is calculated by dividing the sum of truly predicted matrices to the sum of all the matrices calculated as a result of classification. The calculation of precision is formulated by dividing the rightly predicted true classes to the sum of it with wrongly predicted true classes. The calculation of recall is formulated by dividing the rightly predicted true classes to the sum of it with wrongly predicted negative classes. The calculation of sensitivity is formulated by dividing the rightly predicted true classes to the sum of it with wrongly predicted negative classes. The calculation of precision is formulated by dividing the rightly predicted negative classes to the sum of it with wrongly predicted true classes. The calculation of F1 score is formulated by dividing the product of precision and recall to the sum of them.

In the proposed work, the k-fold cross-validation technique is used to prepare the models for testing and prediction purposes. In k-fold cross validation, the dataset is divided into k number of divisions or subsets. One of these divisions is used for training and other one is used for testing. The model gets repeated according to the value of k.[51] The formula for calculating the k-fold cross validation is given in Eq. 6 below:

$$V_f(L) = \frac{1}{K} \sum_{a=1}^{K} M(d_i,\ L^{\sim i}(x_i)) \quad (6)$$

Here, V_f contains the difference between the original value d_i and predicted value $L^{\sim i}$. K here denoted the total number of folds as per which the data points will be put in iteration. In this work, the cross-validation fold is kept at 5 folds in all experiments. In the classification phase, different measures are used which help in constituting a confusion matrix which include True positive rate (TPR), True negative rate (TNR), False positive rate (FPR), and False negative rate (FNR). In this work, TPR and TNR means truly and rightly classified blood smear images. While FPR and FNR means inaccurately and mistakenly classified blood smear images. F1 score denotes the accuracy score of a particular experiment.[52,53]

The experiments are performed on Intel Core i5 with 8GB RAM running on Windows 10 OS. The system houses a 256GB Solid State Drive (SSD) on which the MATLAB 2020a version is installed to perform all the experiments.

Results Evaluation

In the experimental flow of the proposed work, malaria blood smear classification is performed on red blood cells images. A total of four experiments are performed with various inputs and parameter settings. The proposed technique comprises of two pre-trained CNN models SqueezeNet (SQN) and ResNet-101 (RSN-101), a handcrafted feature extractor LBP, and feature optimization algorithm LDA. Experiment 1,2 depict the classification result of standalone SQN and RSN-101 both along with LBP respectively. Experiment 3 shows the classification results after the feature fusion from both deep models and the LBP. The section concludes with experiment 4 highlighting the classification results of complete model which contains merged features from both the deep models and LBP, which are finally reduced and selected with LDA. A total of eight classifiers along with their various kernels are used for feature categorization prominently Logistic Regression (LR), Linear Discriminant (LD), Quadratic Discriminant (QD), Linear SVM (L-SVM), Cubic SVM (CB-SVM), Coarse Gaussian SVM (CG-SVM), Fine KNN (F-KNN), Coarse KNN (CR-KNN) and Weighted KNN (W-KNN). The results of each experiment combination together with appropriate performance evaluation measures are mentioned in coming sections.

Experiment 1

Table 2 shows the classification results of experiment 1, which is performed upon the combination of features obtained by the pre-trained SQN and the handcrafted LBP. Eight distinct classifiers along with their kernels are employed. The cross-validation fold size is kept at 5 folds and the highest accuracy achieved is 97.35% by CB-SVM. The table shows the results yielded by each of the employed classifiers with regards to certain important performance metrics.

Table 2: Experiment 1 Results.

Classifier	Accuracy (%)	Precision (%)	Specificity (%)	Sensitivity (%)	F1 Score
LR	95.84	95.72	95.73	95.95	95.84
LD	96.47	98.27	98.20	94.86	96.54
QD	91.20	88.02	88.74	94.01	90.91
L-SVM	96.46	97.96	97.90	95.10	96.51
CB-SVM	**97.35**	97.85	97.83	96.87	97.36
CG-SVM	95.44	97.65	97.54	93.51	95.53
F-KNN	90.74	94.54	94.09	87.86	91.08
CR-KNN	90.28	97.05	96.59	85.48	90.90
W-KNN	91.95	97.12	96.79	88.02	92.34

It can be seen from Table 2. That CB-SVM achieved an accuracy of 97.35% while LD achieved an accuracy of 96.47%. Thus, CB-SVM stands out in terms of accuracy in case of Experiment 1. Figure 6. Shows the confusion matrix for classifier
with highest accuracy in case of experiment 1. That is CB-SVM.

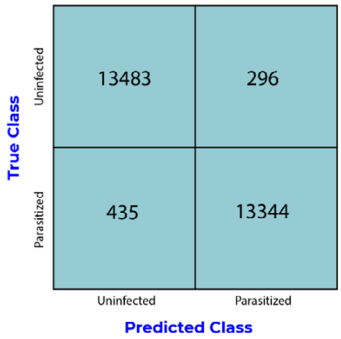

Figure 6: Confusion Matrix for CB-SVM.

Experiment 2

Table 3 shows the results of experiment 2, which used the features learned by pre-trained RSN-101 and the handcrafted LBP while keeping rest of the backdrops same as experiment 1. The cross-validation fold size is kept at 5 folds for this experiment as well and the highest accuracy achieved in this case is 99.46% by the LD classifier.

Table 3: Experiment 2 Results.

Classifier	Accuracy (%)	Precision (%)	Specificity (%)	Sensitivity (%)	F1 Score
LR	99.37	99.59	99.59	99.15	99.37
LD	**99.46**	99.77	99.77	99.16	99.46
QD	95.17	92.86	93.17	97.37	95.06
L-SVM	99.05	99.62	99.61	98.50	99.05
CB-SVM	99.39	99.64	99.64	99.13	99.39
CG-SVM	98.39	99.56	99.55	97.29	98.41
F-KNN	93.00	97.10	96.84	89.75	93.28
CR-KNN	88.99	99.64	99.55	82.15	90.05
W-KNN	93.36	99.06	98.94	88.93	93.72

It can be seen from Table 3. That LD achieved an accuracy of 97.46% while CB-SVM achieved an accuracy of 96.39%. Thus, LD stands out in terms of accuracy in case of Experiment 1. Figure 7. Shows the confusion matrix for classifier with highest accuracy in case of experiment 2. which is LD.

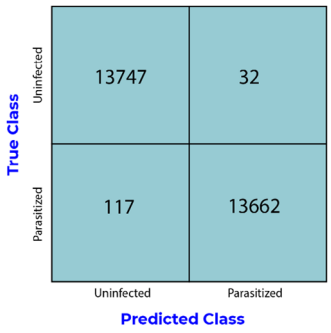

Figure 7: Confusion Matrix for LD.

Experiment 3

After implementing the standalone CNN models in the previous experiments, the next focus is to combine both of their extracted features together to formulate a feature fusion model. Table 4 shows the results of experiment 3 which implements the coalescence of SQN, RSN-101 and the low level feature learner LBP while keeping rest of the parameters same as previous experiments. Same cross-validation size is maintained. The highest accuracy achieved by using this model combination is 99.53% through LD classifier which is better as compared to when standalone models are used.

Table 4: Experiment 3 Results.

Classifier	Accuracy (%)	Precision (%)	Specificity (%)	Sensitivity (%)	F1 Score
LR	99.46	99.62	99.62	99.31	99.46
LD	**99.53**	99.78	99.78	99.29	99.53
QD	93.47	88.36	89.44	98.42	93.12
L-SVM	99.01	99.67	99.67	98.37	99.02
CB-SVM	99.32	99.58	99.58	99.06	99.32
CG-SVM	98.23	99.54	99.52	96.99	98.25
F-KNN	93.78	97.24	97.04	90.94	93.99
CR-KNN	91.16	99.34	99.21	85.38	91.83

It can be seen from Table 4. That LD achieved an accuracy of 97.53% while LR achieved an accuracy of 96.46%. Thus, LD stands out in terms of accuracy in case of Experiment 1. Figure 8. Shows the confusion matrix for classifier with highest accuracy in case of experiment 3. That is LD.

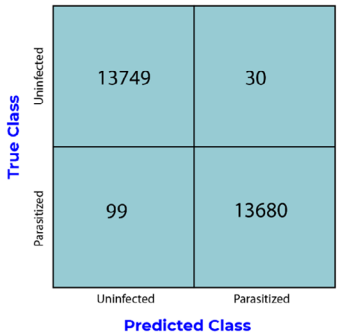

Figure 8: Confusion Matrix for LD.

As it is obvious through experiments 1,2 and 3 that the features learned by two deep models and a low-level

extractor are classified in various combinations where various outcomes are noticed. The fusion based model provides the best classification accuracy as compared to separate deep models as depicted in experiment 3 but this also puts a massive computational burden over the model and the used system where training time and prediction speed are hugely increased. Therefore, LDA optimization algorithm is implemented over the proposed model in the next experiment which decreases complexity, training time and increases prediction speed.

Experiment 4

Table 5 shows the results of experiment 4 where the fused model comprising of two extensive learning frameworks SQN and RSN-101 and native LBP is optimized with the enactment of feature selector LDA. The final combination of features in the fused model are large in number which could cause computational complexity in terms of time and resources usage which is addressed by LDA that selects the most highlighted

Table 5: Experiment 4 Results.

Classifier	Accuracy (%)	Precision (%)	Specificity (%)	Sensitivity (%)	F1 Score
LR	**99.73**	99.76	99.76	99.70	99.73
LD	99.61	99.91	99.91	99.31	99.61
QD	99.68	99.73	99.73	99.62	99.68
L-SVM	99.72	99.79	99.79	99.65	99.72
CB-SVM	68.16	69.68	68.73	67.62	68.63
CG-SVM	99.60	99.91	99.91	99.29	99.60
F-KNN	98.22	98.37	98.37	98.08	98.22
CR-KNN	93.45	95.17	95.00	92.01	93.56
W-KNN	98.32	98.42	98.41	98.23	98.33

It can be seen from Table 5. That LR achieved an accuracy of 97.73% while L-SVM achieved an accuracy of 96.72%. Thus, LR stands out in terms of accuracy in case of Experiment 1.Figure 9. Shows the confusion matrix for classifier with highest accuracy in case of experiment 4. That is LR.

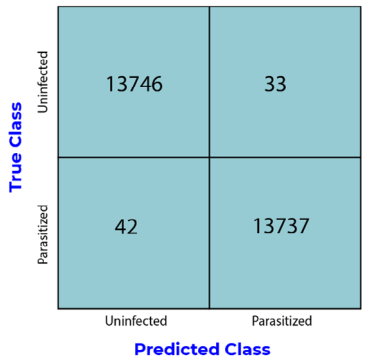

Figure 9: Confusion Matrix for LR.

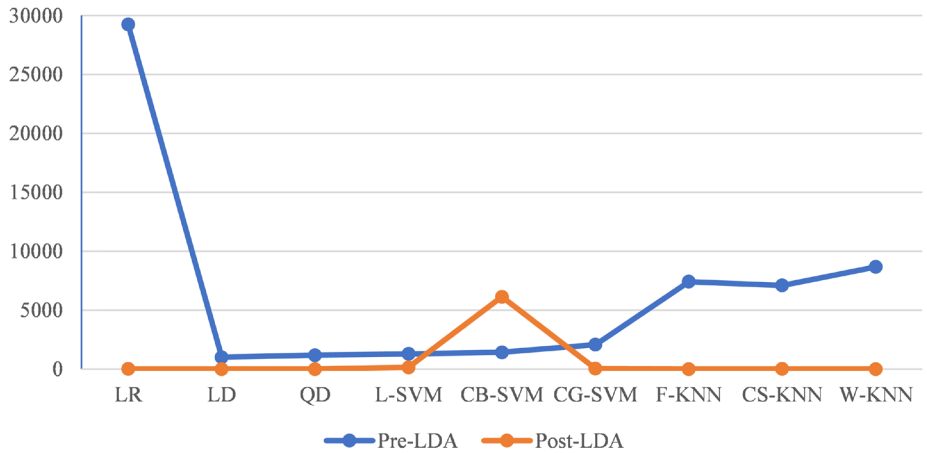

Figure 10: Classifier Training Time Comparison Pre-& Post Optimization.

Figure 10. shows the training time comparison of fused features from both the deep models without any kind of selection and reduction with LDA optimized features. It can be seen that the training time has been greatly reduced after optimizing the features through LDA while as compared to when raw fused features are classified. Figure 11. shows a classification overview with respect to accuracy and training time for the extracted features prior and post optimization. It is quite evident that after the feature selection phase is performed using LDA optimizer, the proposed model provides almost same accuracy but perfectionates itself in terms of time reservation and exertion with training times reducing to an insignificant percentages post feature optimization. This makes the proposed model time efficient to a huge extent while maintaining the best accuracy ratio at the same time.

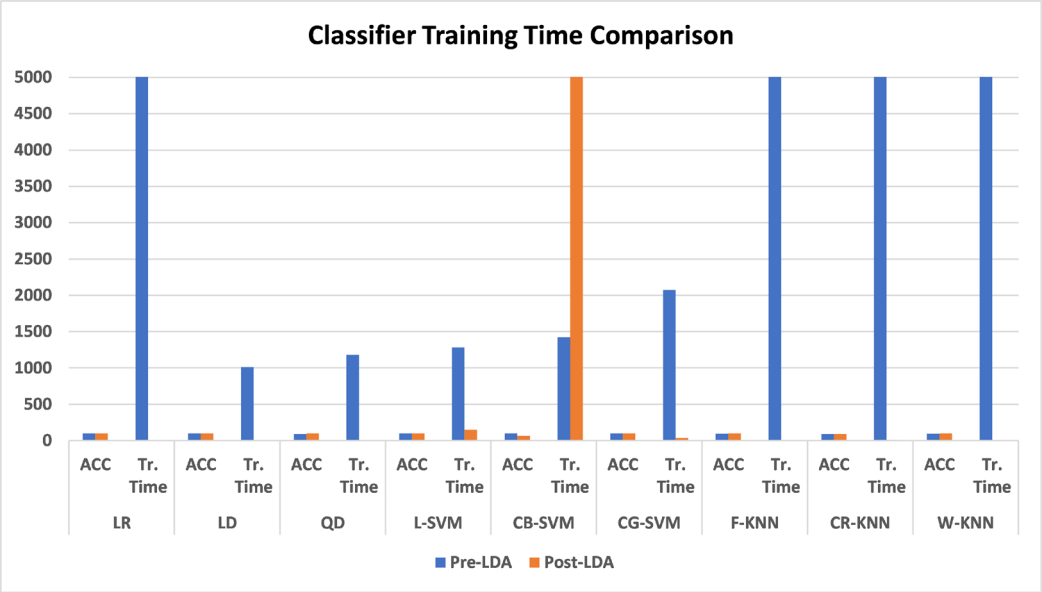

Figure 11: Overview of Accuracy and Time for Proposed Model Pre-& Post Optimization.

Table 6 shows the comparison of latest works proposed on the same dataset with the proposed model. The proposed model performed better on the same dataset with proposed model in terms of accuracy and time.

Table 6: Accuracy Comparison of other Works and Proposed Work.

Reference	Years	Methodology	Accuracy
Masud *et al.*[54]	2020	Custom CNN	97.30%
Sinha *et al.*[55]	2020	ADSN Model based on Deep Conv. Networks	97.47%
Luque *et al.*[52]	2019	Sequential Residual CNN	98%
Quan *et al.*[56]	2020	CNN based CapsNet Model	98.7%
Fuhad *et al.*[57]	2020	Custom 8-layered CNN Model	99.23%
-	**2023**	**Proposed ODMC Model**	**99.73%**

Conclusion

Accurate and on-time diagnosis of malaria is a decisive factor of any affected patient life. Recent advancements in artificial intelligence have provided canonical computer vision-based detection methods for image processing related problems. An ensemble CNN feature fusion-based model ODMC is proposed for the classification of malaria blood smears from red blood cells in this paper which is based on merger of features obtained from profound models RSN-101 and SQN with low level extractor LBP. LDA is implanted for model complexity reduction. Finally, a number of distinctive up to date classifiers along with their kernels are effectuated for classification purpose where maximum accuracy of 99.73% is achieved by the LR classifier which also maintains an efficient time consumption rate. The proposed model excels from previous works in terms of accuracy, prediction speed and training time exertion.

Author Contributions

Talha Imran: Visualization, Validation, Methodology, Formal analysis, Data curation, conceptualization. Saman Iftikhar: Software, Project administration, Formal analysis, Data curation, Conceptualization. Kiran Fatima: Resources, Project administration, Funding acquisition, Formal analysis, Data curation, Conceptualization. Malak ElAmir: Writing - review & editing, Writing - original draft, Visualization, Validation, Supervision, Methodology, Investigation. Noof Abdulaziz Alansari:

Methodology, Investigation, Conceptualization. Ammar Saeed: Writing - review & editing, Writing - original draft.

Data Availability Statement

The dataset is publicly available at Kaggle. https://www.kaggle.com/datasets/iarunava/cell-images-for-detecting-malaria.

Competing Interests Statement

The authors declare no financial interests/personal relationships which may be considered as potential competing interests: No additional information is available for this paper.

Acknowledgement

The authors extend their appreciation to the Arab Open University for funding this work through AOU research fund No. (AOUKSA524008).

References

1. Talapko J, Škrlec I, Alebić T, Jukić M, Včev A. Malaria: The Past and the Present. Microorganisms. 2019; 7(6): 179. doi: https://doi.org/10.3390/microorganisms7060179.
2. Ashton RA, Doumbia B, Diallo D, et al. Measuring malaria diagnosis and treatment coverage in population-based surveys: a recall validation study in Mali among caregivers of febrile children under 5 years. Malar J. 2019; 18(1): 3. doi: https://doi.org/10.1186/s12936-018-2636-3.
3. Espinoza JL. Malaria Resurgence in the Americas: An Underestimated Threat. Pathogens. 2019; 8(1): 11. doi: https://doi.org/10.3390/pathogens8010011.
4. WHO. Global malaria report 2019. World Health Organization Geneva; 2019. Available from: https://www.who.int/publications/i/item/9789241565721.
5. Poostchi M, Silamut K, Maude RJ, Jaeger S, Thoma G. Image analysis and machine learning for detecting malaria. Transl Res. 2018; 194: 36-55. doi: https://doi.org/10.1016/j.trsl.2017.12.004.
6. Muhammad FA, Sudirman R, Zakaria NA, Mahmood NH. Classification of Red Blood Cell Abnormality in Thin Blood Smear Images using Convolutional Neural Networks. J Phys Conf Ser. 2023; 2622(1): 012011. doi: https://doi.org/10.1088/1742-6596/2622/1/012011.
7. Kundu TK, Anguraj DK. Optimal Machine Learning Based Automated Malaria Parasite Detection and Classification Model Using Blood Smear Images. Traitement du Signal. 2023; 40(1): 91-99. doi: https://doi.org/10.18280/ts.400108.
8. Shi L, Guan Z, Liang C, You H. Automatic Classification of Plasmodium for Malaria Diagnosis based on Ensemble Neural Network. In: Proceedings of the 2020 2nd International Conference on Intelligent Medicine and Image Processing. ACM Digital Library; 2020:80-85. doi: https://doi.org/10.1145/3399637.3399641.
9. Pattanaik PA, Mittal M, Khan MZ. Unsupervised Deep Learning Cad Scheme for the Detection of Malaria in Blood Smear Microscopic Images. IEEE Access. 2020; 8: 94936-46. doi: https://doi.org/10.1109/ACCESS.2020.2996022.
10. Shambhu S, Koundal D, Das P. Deep Learning-Based Computer Assisted Detection Techniques for Malaria Parasite Using Blood Smear Images. International Journal of Advanced Technology and Engineering Exploration. 2023; 10(105): 990-1015. doi: https://doi.org/10.19101/IJATEE.2023.10101218.
11. Rajaraman S, Jaeger S, Antani SK. Performance evaluation of deep neural ensembles toward malaria parasite detection in thin-blood smear images. PeerJ. 2019; 7: e6977. doi: https://doi.org/10.7717/peerj.6977.
12. Vijayalakshmi A, Rajesh Kanna B. Deep learning approach to detect malaria from microscopic images. Multimed Tools Appl. 2020; 79(21): 15297-317. doi: https://doi.org/10.1007/s11042-019-7162-y.
13. Abbas N, Saba T, Rehman A, et al. Plasmodium species aware based quantification of malaria parasitemia in light microscopy thin blood smear. Microsc Res Tech. 2019; 82(7): 1198-214. doi: https://doi.org/10.1002/jemt.23269.
14. Abbas N, Saba T, Mohamad D, Rehman A, Almazyad AS, Al-Ghamdi JS. Machine aided malaria parasitemia detection in Giemsa-stained thin blood smears. Neural Comput & Applic. 2018; 29(3): 803-18. doi: https://doi.org/10.1007/s00521-016-2474-6.
15. Yang F, Poostchi M, Yu H, et al. Deep Learning for Smartphone-Based Malaria Parasite Detection in Thick Blood Smears. IEEE J Biomed Health Inform. 2020; 24(5): 1427-38. doi: https://doi.org/10.1109/jbhi.2019.2939121.
16. Santosh T, Ramesh D, Reddy D. LSTM based prediction of malaria abundances using big data. Comput Biol Med. 2020; 124: 103859. doi: https://doi.org/10.1016/j.compbiomed.2020.103859.
17. Liu R, Liu T, Dan T, et al. AIDMAN: An AI-based object detection system for malaria diagnosis from smartphone thin-blood-smear images. Patterns (N Y). 2023; 4(9): 100806. doi: https://doi.org/10.1016/j.patter.2023.100806.
18. Irrigisetty H, Madhavi KR, Prasad VS, Jonna H, Kurlapalli M, Gangadasari HR. Enhancing High-Resolution Malaria Parasite Detection In Blood Smears Using Deep Learning. In: 2024 5th International Conference for Emerging Technology (INCET). IEEE; 2024:1-9. doi: https://doi.org/10.1109/INCET61516.2024.10593540.
19. Somasekar J, Reddy BE. Segmentation of erythrocytes infected with malaria parasites for the diagnosis using microscopy imaging. Comput Electr Eng. 2015; 45: 336-51. doi: https://doi.org/10.1016/j.compeleceng.2015.04.009.
20. Gandhamal A, Talbar S, Gajre S, Hani AF, Kumar D. Local gray level S-curve transformation - A generalized contrast enhancement technique for medical images. Comput Biol Med. 2017; 83: 120-33. doi: https://doi.org/10.1016/j.compbiomed.2017.03.001.
21. Gao G, Wan X, Yao S, Cui Z, Zhou C, Sun X. Reversible Data Hiding With Contrast Enhancement and Tamper Localization for Medical Images. Inf Sci (N Y). 2017; 385-386: 250-65. doi: https://doi.org/10.1016/j.ins.2017.01.009.

22. Grigoryan AM, John A, Agaian SS. Color image enhancement of medical images using alpha-rooting and zonal alpha-rooting methods on 2D QDFT. In: Medical Imaging 2017: Image Perception, Observer Performance, and Technology Assessment. SPIE; 2017:325-33. doi: https://doi.org/10.1117/12.2254889.
23. Yang Y, Zhang W, Liang D, Yu N. A ROI-based high capacity reversible data hiding scheme with contrast enhancement for medical images. Multimed Tools Appl. 2018; 77(14): 18043-65. doi: https://doi.org/10.1007/s11042-017-4444-0.
24. Echegaray S, Bakr S, Rubin DL, Napel S. Quantitative Image Feature Engine (QIFE): an Open-Source, Modular Engine for 3D Quantitative Feature Extraction from Volumetric Medical Images. J Digit Imaging. 2018; 31(4): 403-14. doi: https://doi.org/10.1007/s10278-017-0019-x.
25. Lorenzo-Ginori JV, Chinea-Valdés L, IzquierdoTorres Y, et al. Color Features Extraction and Classification of Digital Images of Erythrocytes Infected by Plasmodium berghei. In: Vera-Rodriguez R, Fierrez J, Morales A, Eds. Progress in Pattern Recognition, Image Analysis, Computer Vision, and Applications: 23rd Iberoamerican Congress, CIARP 2018, Madrid, Spain, November 19-22, 2018, Proceedings 23. Springer; 2019:715-22. doi: https://doi.org/10.1007/978-3-030-13469-3_83.
26. Rundo L, Tangherloni A, Galimberti S, et al. HaraliCU: GPU-Powered Haralick Feature Extraction on Medical Images Exploiting the Full Dynamics of Gray-Scale Levels. In: Malyshkin V, Ed. Parallel Computing Technologies: 15th International Conference, PaCT 2019, Almaty, Kazakhstan, August 19–23, 2019, Proceedings 15. Springer; 2019:304-18. doi: https://doi.org/10.1007/978-3-030-25636-4_24.
27. Wang R, Shi Y, Cao W. GA-SURF: A new speeded-up robust feature extraction algorithm for multispectral images based on geometric algebra. Pattern Recognit Lett. 2019; 127: 11-17. doi: https://doi.org/10.1016/j.patrec.2018.11.001.
28. Ojala T, Pietikainen M, Harwood D. Performance Evaluation of Texture Measures With Classification Based on Kullback Discrimination of Distributions. In: Proceedings of 12th International Conference on Pattern Recognition. IEEE; 1994:582-85. doi: https://doi.org/10.1109/ICPR.1994.576366.
29. Abbasi S, Tajeripour F. Detection of brain tumor in 3D MRI images using local binary patterns and histogram orientation gradient. Neurocomputing (Amst). 2017; 219: 526-35. doi: https://doi.org/10.1016/j.neucom.2016.09.051.
30. Singh C, Walia E, Kaur KP. Color texture description with novel local binary patterns for effective image retrieval. Pattern Recognit. 2018; 76: 50-68. doi: https://doi.org/10.1016/j.patcog.2017.10.021.
31. Zhao H, Zhan ZH, Lin Y, et al. Local Binary Pattern-Based Adaptive Differential Evolution for Multimodal Optimization Problems. IEEE Trans Cybern. 2020; 50(7): 3343-57. doi: https://doi.org/10.1109/tcyb.2019.2927780.
32. Eisa M, ElGamal A, Ghoneim R, Bahey A. Local Binary Patterns as Texture Descriptors for User Attitude Recognition. IJCSNS International Journal of Computer Science and Network Security. 2010; 10(6): 222-29. Available from: http://paper.ijcsns.org/07_book/201006/20100630.pdf.
33. Heikkilä M, Pietikäinen M, Schmid C. Description of Interest Regions With Local Binary Patterns. Pattern Recognit. 2009; 42(3): 425-36. doi: https://doi.org/10.1016/j.patcog.2008.08.014.
34. Du Y, Zhang R, Zargari A, et al. A performance comparison of low-and high-level features learned by deep convolutional neural networks in epithelium and stroma classification. In: Medical imaging 2018: digital pathology. SPIE; 2018:304-09. doi: https://doi.org/10.1117/12.2292840.
35. Abbas A, Abdelsamea MM, Gaber MM. Classification of COVID-19 in chest X-ray images using DeTraC deep convolutional neural network. Appl Intell (Dordr). 2021; 51(2): 854-64. doi: https://doi.org/10.1007/s10489-020-01829-7.
36. Gao F, Wu T, Li J, et al. SD-CNN: A shallow-deep CNN for improved breast cancer diagnosis. Comput Med Imaging Graph. 2018; 70: 53-62. doi: https://doi.org/10.1016/j.compmedimag.2018.09.004.
37. Moriya T, Roth HR, Nakamura S, et al. Unsupervised segmentation of 3D medical images based on clustering and deep representation learning. In: Medical Imaging 2018: Biomedical Applications in Molecular, Structural, and Functional Imaging. SPIE; 2018:483-89. doi: https://doi.org/10.1117/12.2293414.
38. Trivizakis E, Manikis GC, Nikiforaki K, et al. Extending 2-D Convolutional Neural Networks to 3-D for Advancing Deep Learning Cancer Classification With Application to MRI Liver Tumor Differentiation. IEEE J Biomed Health Inform. 2019; 23(3): 923-30. doi: https://doi.org/10.1109/jbhi.2018.2886276.
39. Xu Y, Hosny A, Zeleznik R, et al. Deep Learning Predicts Lung Cancer Treatment Response from Serial Medical Imaging. Clin Cancer Res. 2019; 25(11): 3266-75. doi: https://doi.org/10.1158/1078-0432.ccr-18-2495.
40. Ghosal P, Nandanwar L, Kanchan S, Bhadra A, Chakraborty J, Nandi D. Brain Tumor Classification Using ResNet-101 Based Squeeze and Excitation Deep Neural Network. In: 2019 Second International Conference on Advanced Computational and Communication Paradigms (ICACCP). IEEE; 2019:1-6. doi: https://doi.org/10.1109/ICACCP.2019.8882973.
41. Rust F. Computer Vision and Deep Learning in medical imaging Detecting Covid-19 on chest CT scans.
42. Roslidar R, Saddami K, Arnia F, Syukri M, Munadi K. A Study of Fine-Tuning CNN Models Based on Thermal Imaging for Breast Cancer Classification. In: 2019 IEEE International Conference on Cybernetics and Computational Intelligence (CyberneticsCom). IEEE; 2019:77-81. doi: https://doi.org/10.1109/CYBERNETICSCOM.2019.8875661.

43. Nabavi S, Ejmalian A, Moghaddam ME, et al. Medical imaging and computational image analysis in COVID-19 diagnosis: A review. Comput Biol Med. 2021; 135: 104605. doi: https://doi.org/10.1016/j.compbiomed.2021.104605.
44. Zhang X, Hu W, Chen F, et al. Gastric precancerous diseases classification using CNN with a concise model. PLoS One. 2017; 12(9): e0185508. doi: https://doi.org/10.1371/journal.pone.0185508.
45. Khalifa NEM, Loey M, Taha MHN, Mohamed H. Deep Transfer Learning Models for Medical Diabetic Retinopathy Detection. Acta Inform Med. 2019; 27(5): 327-32. doi: https://doi.org/10.5455/aim.2019.27.327-332.
46. Hassan M, Ali S, Alquhayz H, Safdar K. Developing intelligent medical image modality classification system using deep transfer learning and LDA. Sci Rep. 2020; 10(1): 12868. doi: https://doi.org/10.1038/s41598-020-69813-2.
47. Ali L, Wajahat I, Amiri Golilarz N, Keshtkar F, Bukhari SAC. LDA–GA–SVM: improved hepatocellular carcinoma prediction through dimensionality reduction and genetically optimized support vector machine. Neural Comput & Applic. 2021; 33(7): 2783-92. doi: https://doi.org/10.1007/s00521-020-05157-2.
48. Balakrishnama S, Ganapathiraju A. Linear Discriminant Analysis-A Brief Tutorial. Institute for Signal and information Processing. 1998; 18(1998): 1-8. Available from: https://isip.piconepress.com/publications/reports/1998/isip/lda/lda_theory_v1.1.pdf.
49. Kaggle. Malaria Cells Images Dataset. 2018. Accessed July 20, 2020, Available from: https://www.kaggle.com/datasets/iarunava/cell-images-for-detecting-malaria.
50. Ballabio D, Grisoni F, Todeschini R. Multivariate Comparison of Classification Performance Measures. Chemometr Intell Lab Syst. 2018; 174: 33-44. doi: https://doi.org/10.1016/j.chemolab.2017.12.004.
51. Wong T-T, Yeh P-Y. Reliable Accuracy Estimates from k-Fold Cross Validation. IEEE Trans Knowl Data Eng. 2019; 32(8): 1586-94. doi: https://doi.org/10.1109/TKDE.2019.2912815.
52. Luque A, Carrasco A, Martín A, de Las Heras A. The impact of class imbalance in classification performance metrics based on the binary confusion matrix. Pattern Recognit. 2019; 91: 216-31. doi: https://doi.org/10.1016/j.patcog.2019.02.023.
53. Abdel-Jaber H, Devassy D, Al Salam A, Hidaytallah L, EL-Amir M. A Review of Deep Learning Algorithms and Their Applications in Healthcare. Algorithms. 2022; 15(2): 71. doi: https://doi.org/10.3390/a15020071.
54. Masud M, Alhumyani H, Alshamrani SS, et al. Leveraging Deep Learning Techniques for Malaria Parasite Detection Using Mobile Application. Wirel Commun Mob Comput. 2020; 2020(1): 8895429. doi: https://doi.org/10.1155/2020/8895429.
55. Sinha S, Srivastava U, Dhiman V, Akhilan PS, Mishra S. Performance assessment of Deep Learning procedures on Malaria dataset. Journal of Robotics and Control (JRC). 2021; 2(1): 12-18. doi: https://doi.org/10.18196/jrc.2145.
56. Quan Q, Wang J, Liu L. An Effective Convolutional Neural Network for Classifying Red Blood Cells in Malaria Diseases. Interdiscip Sci. 2020; 12(2): 217-25. doi: https://doi.org/10.1007/s12539-020-00367-7.
57. Fuhad KMF, Tuba JF, Sarker MRA, Momen S, Mohammed N, Rahman T. Deep Learning Based Automatic Malaria Parasite Detection from Blood Smear and its Smartphone Based Application. Diagnostics (Basel). 2020; 10(5): 329. doi: https://doi.org/10.3390/diagnostics10050329.